Middle Distillates Production via Fischer–Tropsch Synthesis with Integrated Upgrading Under Supercritical Conditions

Sihe Zhang, Rui Xu, Ed Durham, and Christopher B. Roberts
Dept. of Chemical Engineering, Auburn University, AL 36849

DOI 10.1002/aic.14493
Published online May 22, 2014 in Wiley Online Library (wileyonlinelibrary.com)

A vertically aligned fixed-bed reactor system with a cascade of three sequential catalyst beds has been used to incorporate Fischer–Tropsch synthesis (FTS) in the first bed, oligomerization (O) in the second bed, and hydrocracking/isomerization (HC or C) in the third bed (FTOC). Compared to gas phase FTS (GP-FT) alone, gas phase FTS with the subsequent upgrading beds (GP-FTOC) is demonstrated to result in a reduction in the olefin selectivity, a reduction in the C_{26+} selectivity, and a marked enhancement in the production of branched paraffins and aromatics. Utilization of supercritical hexane as the reaction medium in supercritical FTS (SC-FT) and supercritical phase FTOC (SC-FTOC) resulted in a significant reduction in both CH_4 selectivity and CO_2 selectivity. Interestingly, significant amounts of aldehydes and cyclo-paraffins were collected in SC-FT and in SC-FTOC, respectively, while not being observed in traditional gas phase operation (both GP-FT and GP-FTOC). © 2014 American Institute of Chemical Engineers *AIChE J*, 60: 2573–2583, 2014

Keywords: multibed reaction system, middle distillates, Fischer–Tropsch synthesis, oligomerization, hydrocracking/isomerization, supercritical phase conditions

Introduction

There has been a great deal of contemporary interest in the utilization of a variety of carbonaceous feedstocks to produce readily usable transportation fuels via synthesis gas (syngas, a mixture of H_2 and CO).[1–7] Specifically, Fischer–Tropsch synthesis (FTS) can be used to convert syngas into hydrocarbon products and oxygenated hydrocarbons.[7–11] FTS is a surface-catalyzed polymerization process that converts *in situ* generated C_1 species monomers into hydrocarbons with a broad range of carbon chain lengths and functionalities.[2,3,12–15] With appropriate separation, upgrading and hydro-processing, these products can be further converted into high-quality fuels and value-added chemicals.[2,16–22] Compared to crude-oil-derived transportation fuels, FT-derived fuels have distinct features including the absence of sulfur and nitrogen, low aromatic concentration, and so forth.[23,24] FTS with conventional supported metal catalysts yields a wide spectrum of hydrocarbons since the product distribution is considered to be governed by the Anderson–Schulz–Flory (ASF) polymerization kinetics, which imposes a limitation on the maximum selectivity for a given hydrocarbon product. To improve the selectivity of the FTS process toward middle distillate range products (C_8—C_{22}), additional upgrading reactions are required. A significant number of studies have focused on two major topics related to improving selectivities toward the middle distillates: (1) modification of the reaction catalysts through the use of bi-/multifunctional catalysts[25–28] and (2) modification of the reaction system by adding further upgrading processes downstream of FTS.[25,29,30] The studies involving catalyst modifications primarily use hybrid catalyst systems, an FTS catalyst (the catalyst support may or may not be modified) and an acid catalyst with/without noble metal doping.[24–27,31–39] Investigations involving upgrading FTS by modification of the reaction system typically make use of a dual bed reactor system that includes the integration of an FTS wax hydrocracking stage in the second bed.[25,29–31]

There have been few investigations that have incorporated oligomerization into the FTS process since most of the studies involving modification of the FTS products are focused primarily on the conversion of heavy hydrocarbons into the middle distillate range. However, implementation of oligomerization into the FTS process could potentially allow the conversion of light olefins into longer fuel range hydrocarbons.[17,40,41]

Improvement of the selectivity of the process toward middle distillate hydrocarbons requires that additional upgrading reactions be included. This study addresses this need through the implementation of a three-bed reactor system (consisting of three sequential fixed-bed reactors) in order to promote the direct production of middle distillate range hydrocarbons from syngas in a single pass arrangement. FTS is performed in the first catalyst bed, thereby generating a range of hydrocarbons of different carbon chain length and functionality (i.e., paraffins, olefins, and oxygenates). The second bed is used for oligomerization to convert light olefins into gasoline and diesel range products (to promote branching and to enhance octane rating and cold-flow properties or

Correspondence concerning this article should be addressed to C. B. Roberts at croberts@eng.auburn.edu.

This article is based on a contribution that was identified by Paul Witt (US Department of Energy) as the Best Presentation in the session "Syngas Production and Gas-to-Liquid Technology" of the 2012 AIChE Annual Meeting in Pittsburgh, PA.

aromatization to enhance density). The third bed is used for cracking and isomerization reactions to convert the heavy product into the middle distillate range and to increase branching.

To achieve the optimum performance within each catalyst bed, this three-bed reactor was arranged consecutively so that the operation parameters of each reactor can be adjusted and maintained individually. A precipitated iron-based FTS catalyst was used in the first FTS bed. Iron-based FTS catalysts offer lower hydrogenation activity than cobalt-based FTS catalysts, which therefore results in higher olefin selectivity in low-temperature FTS.[3] Therefore, using a low-cost precipitated iron-based low-temperature FTS catalyst can provide a more desirable feed (due to higher olefin content) when an oligomerization step is implemented sequentially downstream of the FTS step.

In the second bed, light olefins can be oligomerized into the gasoline (C_5—C_{12}) and diesel (C_{12}—C_{22}) range fractions so as to increase the middle distillates selectivity in a single pass. Amorphous silica alumina (ASA) has been less studied, compared to solid phosphoric acid (SPA) and ZSM-5, and has been proposed by de Klerk to offer promising oligomerization performance.[40] Oligomerization using ASA leads to higher distillate density and product viscosity compared to SPA and ZSM-5, while de Klerk showed that the presence of low levels of oxygenates did not significantly affect productivity.[40,41] Given the promise that ASA offers as an oligomerization catalyst, ASA was chosen to initiate these oligomerization investigations in the second bed of this sequential reactor system.

The third bed of this sequential reactor system is intended to convert long chain FTS hydrocarbons into middle distillate range products through catalytic hydrocracking and isomerization. Common hydrocracking catalysts include Pd- and Pt-based solid acid catalysts.[42–44] It should be noted that there is an inherent competition between hydrogenation–dehydrogenation reactions and the cracking reaction in this system. Since Pd exhibits a weaker hydrogenation–dehydrogenation activity compared to Pt,[45] it can offer a higher cracking activity than Pt.[39] Additionally, Liu et al. reported that Pd-based catalysts showed better catalytic performance maintenance than Pt-based catalysts.[30] As such, Pd has been chosen over Pt as the active metal in initiating these investigations. ASA has been selected as the support material in the following hydrocracking/isomerization investigations due to its high hydroisomerization performance.[39,40,46] Pd-loaded ASA (1.0 wt % prepared by wetness impregnation method) has been selected as the catalyst in the third reactor bed in order to investigate the subsequent hydrocracking/isomerization step. The hydrocracking and isomerization bed with Pd/ASA catalyst is intentionally placed last in this sequence of reaction steps. The Pd/ASA is also a functional hydrogenation and hydroconversion catalyst, and as such, this catalyst can convert olefins into their hydrogen-saturated state (i.e., paraffin). Therefore, if this hydrocracking and isomerization step was placed before the oligomerization bed, no potential oligomerization would occur because of the feed having been already hydrogenated.

There have been a very large number of research studies that have utilized supercritical fluids (SCF) in reactions,[2,47–49] extraction[50] and material processing studies,[51] to name a few. Compared to traditional FTS, the advantages of FTS under supercritical phase conditions (SC-FT) using a SCF as the reaction medium have been studied and reported by several researchers.[2,13–15,25,52–62] There are several advantages to the utilization of supercritical solvents in FTS, including:

1. The elimination of interphase transport limitations can lead to enhanced reactivity toward the desired products[63];
2. The heavy hydrocarbons can be extracted *in situ* from the catalyst surface resulting from the high solubility in the supercritical phase[2,55,63,64];
3. The desorption of primary products can be enhanced prior to being converted through secondary reactions, as an example a higher α-olefin selectivity is observed in SC-FT compared to gas phase FTS[15,55,58,60];
4. Supercritical solvents can provide superior heat transfer compared to gas phase FTS (FTS is highly exothermic in nature).[15,55,64]

It has been consistently shown that the presence of the supercritical solvent can afford the opportunity to suppress methane formation[15,55,65–67] in SC-FT due to suppression of the methanation reaction as a result of improved thermal management in the supercritical solvent.[15,58,68] Suppressed CO_2 selectivity was reported in SC-FT by Davis' group[55] and Roberts' group[14] using a cobalt-based FT catalyst and an iron-based FTS catalyst, respectively. In SC-FT, olefin selectivity at the lower carbon numbers has been reported to decrease[58,69] or was not affected,[15] while olefin selectivity at the higher carbon numbers showed an increasing trend.[55,60,69,70] In this study, supercritical hexanes (a mixture of hexane isomers) has been utilized as a reaction medium in order to provide better heat management, improved product solubility in the bulk reaction media, and enhanced catalyst maintenance.

This article examines the effect of integrated upgrading reactions on primary FTS products in a three-bed reactor system, which allows FTS, oligomerization, and cracking/isomerization stages to occur sequentially. This study compares the performance of this multibed reactor system under both gas phase and supercritical phase operation.

Experimental

The precipitated iron-based catalyst is synthesized as follows: deionized ultrafiltered (DIUF) water (Fischer W2-4) was used to dissolve iron nitrate nonahydrate $Fe(NO_3)_3{\cdot}9H_2O$ (Sigma-Aldrich 216828-500G, CAS# 77-61-8) and zinc nitrate hexahydrate $Zn(NO_3)_2{\cdot}6H_2O$ (Sigma-Aldrich 228737-100G, CAS# 13778-30-8) to make a 1M solution and 0.1M solution, respectively. The reducing agent used was a saturated ammonium carbonate $(NH_4)_2CO_3$ (Sigma-Aldrich 207861-100G, CAS# 506-87-6) solution. The mixture of iron nitrate solution and zinc nitrate solution was added continuously at a rate of approximately 2 mL/min into 30 mL DIUF water with agitation (1000 rotations per min). The temperature was held constant by a water bath at 80°C ($\pm$2°C). The pH value was maintained around 7.0 ($\pm$0.5, measured by a Denver Instrument UB-10 pH meter) by the manual addition of saturated ammonium carbonate solution. When the total volume of precipitate and solution was around 1 L, reagents addition was stopped and the solution temperature was maintained at 80°C ($\pm$2°C) with continuous stirring to age the precipitate for 1 h. After aging, the solution and precipitate was allowed to cool to near room temperature. Then, vacuum filtration was applied to the slurry, and the filtered cake was reslurried in DIUF water and stirred to dissolve leftover ions into the water, and then the slurry was vacuum filtered again. This "precipitate washing" process was repeated three times. The filter cake was then

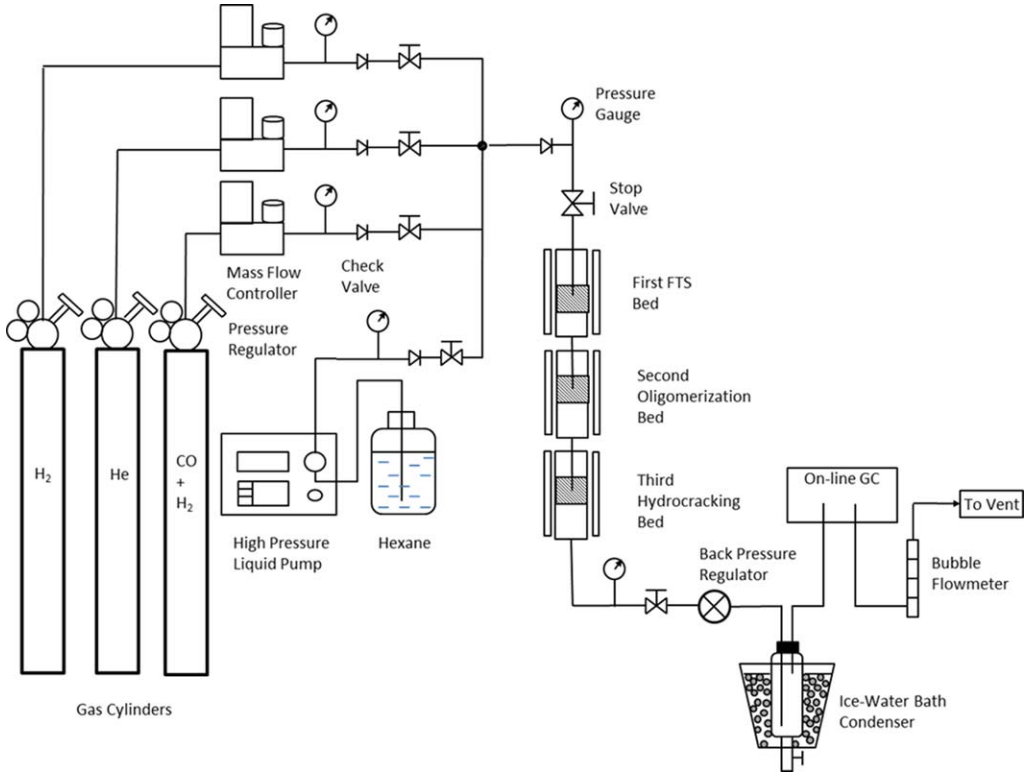

Figure 1. Schematic diagram of the three-bed catalytic reactor system for FTS with subsequent oligomerization and hydrocracking/isomerization stages.

[Color figure can be viewed in the online issue, which is available at wileyonlinelibrary.com.]

manually broken up using a glass rod in an evaporation dish and dried overnight at 80°C. The dried precipitate was calcined (3 g per batch) in a tube furnace with flowing air (15–20 mL/min) at atmospheric pressure. The furnace temperature was programmed to ramp at 5°C/min from room temperature to 400°C. It was held for 4 h at 400°C, and then cooled to room temperature (RT) at 5°C/min. The pore volume of the precursor was measured by addition of DIUF water until it appeared pasty (while measuring the added mass of water). Knowing the water density at the room temperature, the total volume of added water and the pore volume can be determined. The paste was then dried at 80°C. The incipient wetness method was used for copper promotion and potassium promotion. The copper promotion was done by addition of copper nitrate trihydrate $Cu(NO_3)_2{\cdot}3H_2O$ (Sigma-Aldrich 223395-100G, CAS# 3251-23-8) solution. The solution was prepared based on the total pore volume of a certain amount of the aforementioned catalyst and a ratio of 0.01 mol Cu per 1 mol Fe. After the addition of this solution by agitation with a stir rod, the catalyst was then dried and calcined as described above. Similarly, based on the total pore volume of a certain amount of the aforementioned catalyst and a molar ratio of 0.02 mol K per 1 mol Fe, the potassium carbonate (Sigma-Aldrich 209619-100G, CAS# 584-08-7) solution with a proper concentration was prepared. After the copper promotion, potassium was loaded on the catalyst by adding the potassium solution, where the mixture was stirred by a glass rod, and the solution was then dried and calcined following the same procedures as described above. The ASA was obtained from Sigma-Aldrich (343358-1KG, grade 135) and the 1 wt% Pd/ASA catalysts was prepared by the wetness impregnation method. The palladium doping was done by addition of palladium nitrate dihydrate $Pd(NO_3)_2{\cdot}2H_2O$ (Sigma-Aldrich Fluka 76070-1g, CAS# 10102-05-3) solution (0.1 g Pd in 30 mL solution). After addition of this solution to ASA on a mass ratio of 1 g Pd per 99 g ASA at an agitation rate of 200 rpm, the catalyst was aged at room temperature for 24 h. The catalyst was then dried at 100°C for 12 h under air flow. Subsequently, the catalyst was calcined at 500°C for 5 h. The oven temperature was programmed to ramp at 5°C/min to 500°C and held for 5 h, then the oven was cooled to room temperature at 5°C/min.

The three-bed reactor system has been designed to allow the beds to operate at different temperatures so as to optimize each reaction stage, although, isobaric operation is required. A diagram of the three-bed reactor system for FTS with product upgrading under the supercritical phase conditions is shown in Figure 1.

Helium gas (Airgas, ultra high purity) was used during the system pressure test, reaction startup and shut down. Syngas (Airgas, vol%: N_2: CO: H_2 = 1.5: 36.5: 62) was fed into the reaction system by a mass flow controller. In the case of supercritical phase operation, hexanes (Fischer, HPLC grade, CAS# 110-54-3) were used as the SCF reaction media and were delivered into the reaction system using an HPLC pump at a flow rate of 1 mL/min. The syngas and hexanes were mixed in a static mixer and the mixture was initially heated in the preheating zone. The reactant (and the SCF media in the case of supercritical phase operation) entered the top of the tubular fixed-bed reactor and then was passed through each reaction bed sequentially. The reactor effluent was passed through heated tubing to the back pressure regulator (BPR, Straval Valves, model BPH0502T) which was

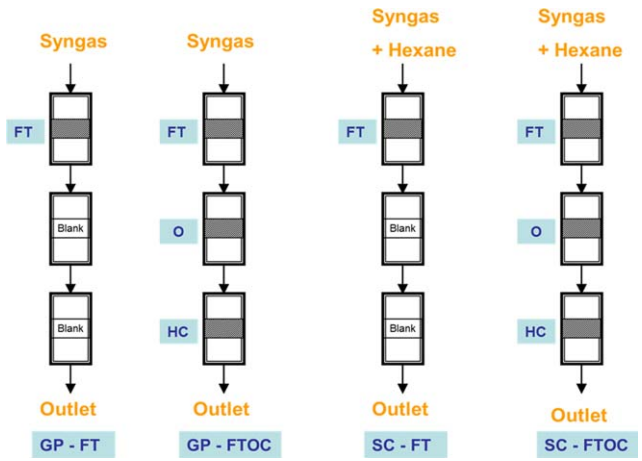

Figure 2. Catalyst loading configurations and reactant/solvent feed schemes for gas phase and supercritical phase FTS with and without subsequent oligomerization and hydrocracking/isomerization stages.

[Color figure can be viewed in the online issue, which is available at wileyonlinelibrary.com.]

used to control the system pressure. The effluent was then passed through heated tubing to a cold trap. The cold trap was cooled by an ice–water mixture. The condensable products were accumulated in the cold trap and were manually collected and tested periodically by injecting them into a gas chromatograph with a flame ionization detector (GC-FID, Varian GC 3300 with a DB-5 capillary column) and a GC-MS (Waters). The uncondensable gas mixture (syngas residue and light products) left the cold trap and was passed through a 10-port injection valve for periodic injection into a gas chromatograph with a thermal conductivity detector (GC-TCD, SRI MultiGas Analyzer #1). The gases were then passed through a bubble meter, which allowed for the measurement of the real-time gas effluent volumetric flow rates. The gas effluent was then vented into the fume hood.

Figure 2 shows the catalyst loading for each bed during each different operation. The experiments were performed in four modes of operation: gas phase FTS (GP-FT), supercritical phase FTS (SC-FT), gas phase FTS with product upgrading (GP-FTOC), and supercritical phase FTS with product upgrading (SC-FTOC). One gram of precipitated Fe/Zn/K/Cu (molar ratio, Fe:Zn:Cu:K = 1:0.1:0.01:0.02) FTS catalyst in the first FTS bed, 1 g of ASA (Sigma-Aldrich, 343358-1KG) catalyst in the second bed, and 1 g of Pd/ASA (1.0 wt %) hydrocracking/isomerization catalyst in the third bed were used for the corresponding experiments. Before the reactions were conducted, a catalyst reduction step was performed using a H_2 flow of 50 SCCM at the desired reduction temperature for each reaction bed. The H_2 flow was controlled before it entered the first bed and then passed through the second bed and the third bed, consecutively. As such, the reduction effluent from the previous bed passed through the following beds sequentially. The reduction temperature was ramped from room temperature to 270°C (the first FTS bed), 400°C (the second oligomerization bed), and 400°C (the third hydrocracking/isomerization bed) at a rate of 5°C/min, respectively. The bed temperature was held at the desired temperature value for 10 h. After the reduction, all the catalyst beds were cooled to room temperature. Hydrogen flow was then switched to helium flow at a rate of 100 SCCM in order to build up the system pressure by adjusting the BPR. After the system pressure was achieved at the set point, the syngas flow was introduced into the system at a controlled flow rate of 50 SCCM (H_2:CO ratio of 1.7:1, vol.) at the inlet for each of the experiment. The reaction temperature for each bed was: FTS at 240°C, oligomerization at 200°C and hydrocracking/isomerization at 330°C. Since the temperature is maintained at a different value in each reactor bed, it is noted that the corresponding flow rate would change in each bed accordingly. The system pressure was uniform for all three reaction beds during each operation. The system pressure for GP-FT was 17.2 bar, for GP-FTOC was 35 bar (the pressure is preferred by the upgrading reactions and the syngas pressure is 35 bar in this case) and 76 bar for all supercritical phase operations (with a hexanes flow rate of 1 mL/min while maintaining the partial pressure of syngas at 17.2 bar by ensuring a constant flow rate of syngas). Table 1 shows the catalyst loading and reaction conditions for each operation. The carbon chain propagation probability (α) of the products was determined from an ASF plot. Based on a stepwise carbon chain growth assumption, α is independent of the carbon chain length, and the equation is

$$\log(W_i/i) = i\log\alpha + \log((1-\alpha)/\alpha)$$

where the mass fraction of a chain of length i, W_i, can be measured from GC analysis. The value of α can be determined from the slope of the plot of log (W_i/i) against i.[23] In this study, the determination of the value of α was performed using liquid products with carbon numbers between C_5 and C_{32}.

Results and Discussion

As shown in Figure 3, under supercritical phase conditions, the carbon monoxide (CO) conversion dropped slowly

Table 1. Reaction Conditions and Catalysts Used in the Fischer–Tropsch Synthesis With and Without Subsequent Oligomerization and Hydrocracking/Isomerization Stages Under Gas Phase and Supercritical Phase Conditions

Reaction Conditions					
Operation Phase	Reaction Stages	T (°C) (FT/O/C)	P (Bar)	Synthesis Gas Flow Rate (SCCM)[a]	Catalysts Loading (FT/O/C)
Gas Phase	FT[b]	240/240/240	17.2	50	1g Fe[d] / - / -
Gas Phase	FTOC[c]	240/200/330	35.0	50	1g Fe[d]/1g ASA/1g Pd-ASA
Supercritical Phase[e]	FT[b]	240/240/240	76	50	1g Fe[d] / - / -
Supercritical Phase[e]	FTOC[c]	240/200/330	76	50	1g Fe[d]/1g ASA/1g Pd-ASA

[a]Syngas H_2:CO:N_2 ratio = 62.0:36.5:1.5, SCCM: standard cubic centimeter per minute, GHSV:84.04 h^{-1}.
[b]FT stands for Fischer–Tropsch synthesis.
[c]FTOC stands for Fischer–Tropsch synthesis with subsequent oligomerization and hydrocracking/isomerisation.
[d]Fe-based FT catalyst, with a molar ratio of Fe:Zn:K:Cu = 1:0.1:0.02:0.01.
[e]Supercritical media is hexanes with a media to syngas ratio of 3.5:1, supercritical media flow rate is 1 mL/min.

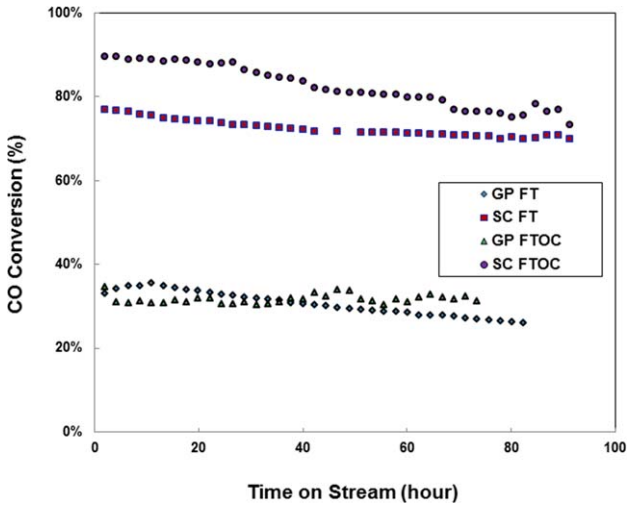

Figure 3. CO conversion as a function of time on stream for gas phase FTS (GP-FT), gas phase FTS with oligomerization and hydrocracking/isomerization (GP-FTOC), supercritical phase FTS (SC-FT), and supercritical phase FTS with oligomerization and hydrocracking/isomerization (SC-FTOC).

[Color figure can be viewed in the online issue, which is available at wileyonlinelibrary.com.]

as a function of time on stream (over a 100+ hours period). The CO conversion under these SC conditions was distinguishably higher (ca. 75%) than that obtained in the gas phase studies (ca. 35%) while the syngas flow rate (50 SCCM) and the syngas composition (H_2:CO = 1.7:1) were held constant in each of the GP-FT, SC-FT, GP-FTOC, and SC-FTOC cases.

The syngas partial pressure in the GP-FT, SC-FT, and the SC-FTOC experiments were held constant at 17.2 bar, while the syngas partial pressure in the GP-FTOC was maintained at 35 bar.

The partial pressure in this study was calculated based on the mathematical definition of partial pressure, $P_i = y_i * P$, in which y_i is the mole fraction of the i species and P is the total pressure. The mole fraction was calculated from the molar flow rates of syngas and hexanes, which was determined separately from the volumetric flow rate measured during a blank test when all the settings and reaction conditions were kept the same.

The contribution from the effect of pressure on the CO conversion in FT reactions is considered negligible. First, under the gas phase conditions, Sasol has reported that at a constant gas velocity the conversion are independent of pressure in their fixed-bed reactors, so they operate the reactors at a high pressure (27–45 bar).[2,23] Therefore, the increase in the pressure from 17.2 bar in GP-FT to 35 bar in GP-FTOC should have insignificant effect over the CO conversion in FT reactions. Second, by maintaining the syngas partial pressure at a consistent value, the CO conversion in FT was proven to be independent of the system total pressure. Lang et al. reported that by introducing N_2 as a balance gas to increase the system total pressure to SC-FT level while maintaining the syngas space velocity the same as in GP-FT, the syngas conversion was the same and the CO conversion was similar.[69] As a result, the effect of the total pressure on CO conversion is not a contributing factor toward the difference in the observed CO conversion between SC-FT and GP-FT, while maintaining the syngas partial pressure constant at 17.2 bar.

There are several possible reasons for the high CO conversion during the supercritical phase experiments compared to the gas phase experiments. One potential reason is that the supercritical phase affords the ability to perform *in situ* product extraction from the FT catalyst's surface, thereby improving the availability of catalytic active sites thus enhancing the reaction rate (which is proportional to the availability of catalytic active sites).[9,71,72] As such, more CO (as well as H_2) would react on the catalyst's surface, thereby enhancing the CO conversion with all other conditions being held constant. Another possibility is that during the startup period of the FTS reaction, a tremendous amount of reaction heat is released once the FTS reaction conditions (temperature and pressure) are achieved since the FTS reactions are so highly exothermic. In gas phase operation, the local heat removal rate may not be sufficient such that catalytic hot spots can be generated which would inherently lead to catalyst sintering[73–75] and fouling (deposition of inactive carbonaceous compounds such as amorphous carbon, graphitic carbon, coke)[76–80] and thus loss of surface area and active catalyst sites.[7,81] As a result, catalyst deactivation may have occurred due to a loss of catalyst active sites before steady-state operation was achieved in GP-FT and GP-FTOC. However, in the supercritical phase operation, a considerable amount of reaction heat can be efficiently transferred due to the presence of the bulk supercritical reaction media which basically serves as a thermal sink.[68] As a result, the catalyst would not deactivate in the very initial period of the reaction as drastically under SC-FT conditions and SC-FTOC conditions.

The CO_2 selectivity obtained during SC-FT (ca. 17%) and SC-FTOC (ca. 13%) operation was lower than in the GP-FT (ca. 23%) and GP-FTOC (ca. 32%) operation (note that the CO conversion was also different), as shown in Figure 4. This result is consistent with our group's previous investigations of SC-FT in that the CO_2 selectivity is decreased

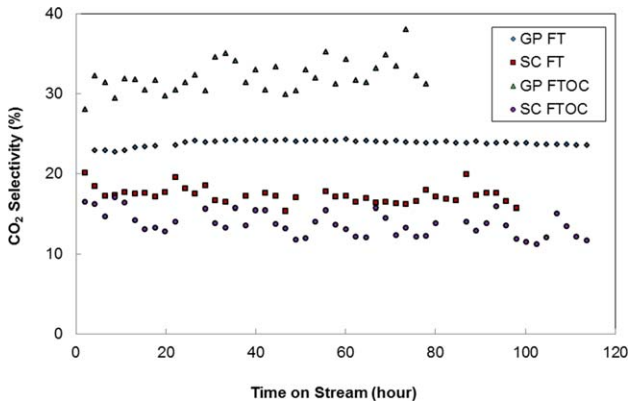

Figure 4. CO_2 selectivity as a function of time on stream for gas phase FTS (GP-FT), gas phase FTS with oligomerization and hydrocracking/isomerization (GP-FTOC), supercritical phase FTS (SC-FT), and supercritical phase FTS with oligomerization and hydrocracking/isomerization (SC-FTOC).

[Color figure can be viewed in the online issue, which is available at wileyonlinelibrary.com.]

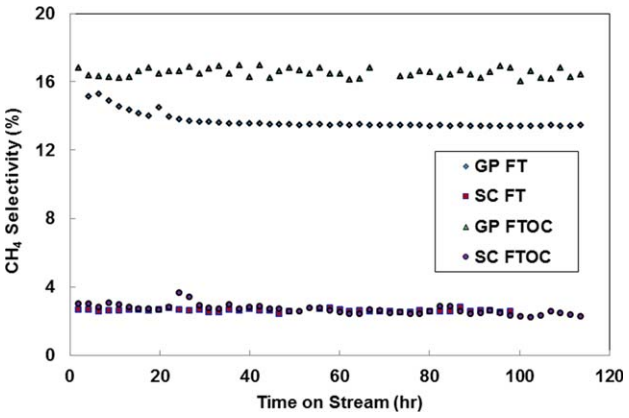

Figure 5. CH_4 selectivity as a function of time on stream for gas phase FTS (GP-FT), gas phase FTS with oligomerization and hydrocracking/isomerization (GP-FTOC), supercritical phase FTS (SC-FT), and supercritical phase FTS with oligomerization and hydrocracking/isomerization (SC-FTOC).

[Color figure can be viewed in the online issue, which is available at wileyonlinelibrary.com.]

relative to GP-FT.[14] Again, this can be attributed to the better heat management (so as to prevent the formation of the hot spots) in the supercritical phase operation thereby suppressing side reactions that affect CO_2 generation.[15,58,68] In addition, the CO_2 selectivity did not show an increasing trend as a function of time on stream (over a 100+ hour period) in the SC-FT and SC-FTOC operations, which is different than that observed in the GP-FT and GP-FTOC operations where there is a modest increase in CO_2 selectivity with time on stream. This observation also suggests that the side reactions were suppressed in the supercritical phase operations compared to the gas phase operations.

The partial pressure of water has a significant inhibiting function over iron-based FT reactions.[23] Fujimoto and coworkers[70] found that the water extraction property by supercritical hexane is proportional to the hexane partial pressure. Under supercritical phase conditions, the water solubility in the supercritical solvent has been greatly enhanced, which leads to higher water extraction and alleviated residence time of water on active sites. As such, the inhibition by water over FT reaction rate by occupancy of active sites is undermined, resulting in an enhanced FT activity. The enhanced water removal from iron active sites at the presence of supercritical hexanes can be another contributor to the higher CO conversion in SC-FT. Meanwhile, the water–gas shift reaction was suppressed due to the decreased water availability on surface iron sites, thus a decreased CO_2 selectivity under supercritical phase conditions.

The methane selectivity was low in both of the supercritical phase operations, below 4%, as shown in Figure 5. Methanation and cracking reactions are promoted by high-temperature operation, and as such, temperature uniformity within the catalytic reaction beds is important in suppressing methane formation.[15,55,58,65,66] The results in Figure 5 indicate that better heat management is obtained in supercritical phase operations as a result of the integration of the supercritical solvent into the FTS and FTOC processes.

In both of the supercritical phase operations, CH_4 and CO_2 selectivity were reduced compared to GP-FT and GP-FTOC indicating that more carbon from CO was converted into heavier hydrocarbons, particularly in light of the higher CO conversion. Table 2 provides a summary of the experimental results of the GP-FT, GP-FTOC, SC-FT, and SC-FTOC studies. It is noted that the CO conversion, CH_4 and CO_2 selectivity listed in Table 2 are average values over the whole operation period. In addition, in the case of GP-FTOC, SC-FT, and SC-FTOC, alcohol selectivity was determined to be negligible (compared to the other types of products obtained under the same reaction conditions) based on the very small GC peak areas obtained. As such, the alcohol selectivity was not included in the table. The SC-FT branched paraffin selectivity was not included for the same reason. The collection of aldehydes, aromatics, and cycloparaffins were uniquely observed in SC-FT, GP-FTOC, and SC-FTOC, respectively. The selectivities of each of these products are shown in Table 2 according to the operating conditions under which they were observed.

Table 2. CO Conversion and Product Selectivities from Fischer–Tropsch Synthesis With and Without Subsequent Oligomerization and Hydrocracking/Isomerization Stages Under Gas Phase and Supercritical Phase Conditions

Operation Phase	Gas Phase	Gas Phase	Supercritical Phase	Supercritical Phase
Reaction Stages	FT[c]	FTOC[d]	FT[c]	FTOC[d]
X CO (%)[a]	31.5	33	75	84
S CO_2 (%)[b]	23	32	17	13
S CH_4 (%)	14	17	3	3
S C_2—C_4 (%)	13.5	9.5	2.1	3.7
S C_5—C_{11} (%)	27.5	12.2	23.8	27.5
S C_{12}—C_{22} (%)	21.3	26.8	40.5	42.7
S C_{22}+ (%)	0.6	2.3	13.6	10.1
S Normal Paraffin (% of C_{5+} products)	24.0	47.9	57.6	53.8
S Olefin (% of C_{5+} products)	45.6	10.5	18.6	30.5
S Branched Paraffin (% of C_{5+} products)	16.3	31.2	NA	5.3
S Alcohol (% of C_{5+} products)	14.8	NA	NA	NA
S Aldehyde (% of C_{5+} products)	NA	NA	23.6	NA
S Aromatics (% of C_{5+} products)	NA	10.4	NA	NA
S cyclo-Paraffin (% of C_{5+} products)	NA	NA	NA	10.3

[a]X stands for conversion.
[b]S stands for selectivity.
[c]FT stands for Fischer–Tropsch synthesis.
[d]FTOC stands for Fischer–Tropsch synthesis with subsequent oligomerization and hydrocracking/isomerisation.
NA: signal not sufficient for GC quantification.

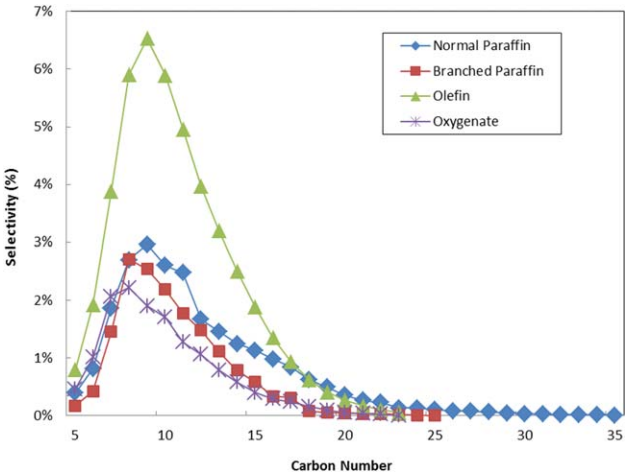

Figure 6. Liquid products selectivities from gas phase FTS (GP-FT).

[Color figure can be viewed in the online issue, which is available at wileyonlinelibrary.com.]

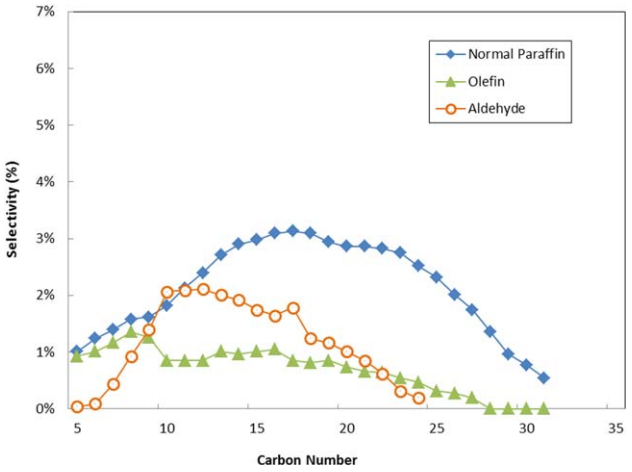

Figure 7. Liquid products selectivities from supercritical phase FTS (SC-FT).

[Color figure can be viewed in the online issue, which is available at wileyonlinelibrary.com.]

A high-propagation probability (α value of 0.94) was observed in SC-FT, as determined by the analysis of the liquid products using GC-FID and GC-MS. This α value is higher than that obtained in the GP-FT (α value of 0.78). This result is in keeping with literature that indicates that the liquid products shift toward the heavy hydrocarbon range under supercritical phase conditions.[15,55,64] Figures 6 and 7 present product selectivities as a function of carbon number for GP-FT and SC-FT, respectively. These results indicate that using the SCF as the reaction medium can promote the carbon chain growth during the FT synthesis.

Consistent with our previous experience in operating SC-FT using an iron-based catalyst, a significant concentration of aldehyde (23.6%) was detected in the liquid products (rather than other oxygenates typically obtained from GP-FT such as alcohols).[14] Our previous results show that these aldehydes are actually intermediates that are generated in the FTS reactions, which can be further converted to other oxygenates or olefins depending on various factors including residence time, catalyst acidity, and operating conditions (Durham et al. submitted).[14] We have found that the enhanced solubility afforded by the use of the SCF as the reaction medium allows these aldehyde intermediates to be efficiently solvated by the supercritical hexanes and extracted from the catalyst as one of the reaction products. Durham et al. illustrated that aldehydes are primary products on an Fe-based catalyst under these SC-FT conditions. They can then be further converted to other oxygenates and olefins (where the olefins can remain as olefins or can be subsequently transformed into paraffins through secondary reactions).[14] A detailed description of the aldehyde incorporation mechanism as a primary FT product in SC-FT is provided elsewhere.[14] The mechanisms that underpin this aldehyde formation are a continuing focus of investigation in our lab.

Hydrocarbon product selectivity (expressed as mole percentage of a given compound or a group of compounds), and CO conversion obtained in these four experiments are shown in Table 2. The syngas flow rate for each of these four experiments was kept constant at the reactor inlet at 50 SCCM in order to maintain the same apparent residence time in the first bed.

After introducing the catalytic oligomerization and hydrogenation reaction beds, the olefin selectivity was greatly reduced in GP-FTOC (Figure 8) compared to GP-FT (Figure 6). As shown in Table 2, the olefin selectivity for the C_{5+} liquid products decreased from 45.6% in GP-FT to 10.5% in GP-FTOC. In GP-FT, terminal olefins are predominant, while in GP-FTOC, internal olefins (middle olefin, etc) are also observed. The introduction of the oligomerization bed and the hydrocracking bed effectively modified the total olefin yield, thus, the olefin concentration is greatly reduced in the GP-FTOC products in which case the olefin concentration can better meet the olefin content necessary in certain fuel regulations.[82,83]

Figure 7 shows the liquid product distribution of SC-FT. As shown in Table 2, the olefin selectivity in SC-FT was around 18.6%, which was significantly less than that in GP-FT (45.6%). However, recall that the aldehyde selectivity was 23.6% under these conditions, and, in light of the work of Durham et al.,[14] there appear to be aldehydes (which are

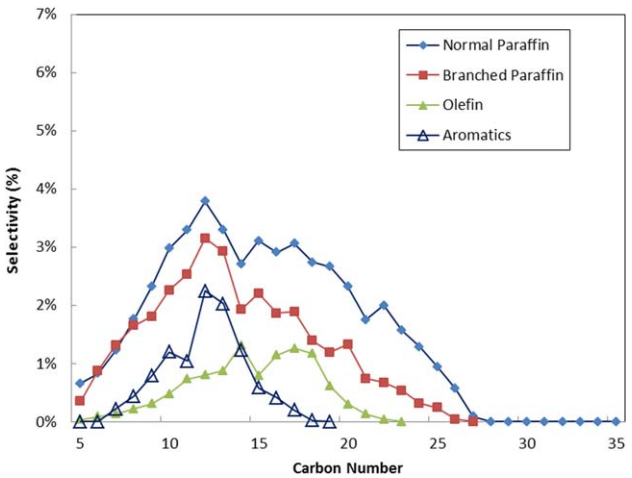

Figure 8. Liquid products selectivities from gas phase FTS with subsequent oligomerization and hydrocracking/isomerization stages (GP-FTOC).

[Color figure can be viewed in the online issue, which is available at wileyonlinelibrary.com.]

produced as the primary product) that have not been converted to olefins under these SC-FT conditions. We note that the sum of the olefin selectivity and the oxygenate selectivity in this SC-FT experiment ($S_{olefin} + S_{aldehyde} = 42.2\%$, not shown in Table 2) was about 18% less than the value from the GP-FT experiment ($S_{olefin} + S_{alcohol} = 60.4\%$, not shown in Table 2). In addition, the paraffin selectivity (either normal paraffin or the sum of the normal paraffin and the branched paraffin) in the SC-FT experiment is higher than that in the GP-FT experiment, as shown in Table 2. All together, the data show that hydrogenation is enhanced under these SC-FT conditions when compared to GP-FT. This observation is consistent with the fact that supercritical reaction solvents have been exploited for elimination interphase gas–liquid mass transport resistances so that it is possible to perform solid-catalyzed hydrogenation with enhanced productivity.[13]

Moreover, due to the enhanced solubility and mass transport that can occur under supercritical phase conditions (compared to gas phase operation), the reaction intermediates can more readily readsorb on catalytic active sites therefore bringing about further carbon chain growth, and thus higher α value in SC-FT compared to GP-FT.[66] The bigger the carbon number of the reaction intermediates, the longer residence time (as a result of slower diffusion rate) they will have within the catalysts thereby resulting in a higher probability of being hydrogenated.[68] Overall, the product distribution shifts to longer chain hydrocarbons in SC-FT compared to that in GP-FT, which is consistent with general observations that have been made in supercritical phase FTS by several research groups.[2,55,63] It is worth noting that both enhanced products extractability (desorption) and products readsorption can result from utilization of SCF solvents, although there should be a balance which is dependent on the reaction conditions.

Figures 8 and 9 exhibit the liquid product distribution of GP-FTOC and SC-FTOC, respectively. De Klerk reported that at 60 bar the oligomerization reaction using an ASA catalyst showed higher activity and better activity maintenance than that at 40 bar.[40] If only based on De Klerk's observation (in a gas phase fluidized bed), the ASA-catalyzed oligomerization conversion would be expected to be higher in supercritical phase operation than that in gas phase since the system total pressure is higher. However, the results from SC-FTOC in Figure 9 show that the use of the supercritical phase reaction media resulted in a higher selectivity toward C_{5+} olefins (30.5%) compared to GP-FTOC conditions (10.5%), noting that the CO conversions were different with values of 75% and 31.5%, respectively. In addition, the olefin selectivity for the C_{5+} liquid products decreased from 45.6% in GP-FT to 10.5% in GP-FTOC while it increased from 18.6% in SC-FT to 30.5% in SC-FTOC.

This higher olefin selectivity in SC-FTOC can result from olefinic products being generated from the cracking/isomerization reactions (as reaction intermediates as discussed below). This result suggests that the positive effect of pressure on ASA catalyzed oligomerization, if any, is compensated for by the enhancement in cracking/isomerization and the elevated extraction of reaction intermediates under supercritical conditions (these intermediates are olefins in the case of hydrocracking/isomerization). Thus, the results from SC-FTOC exhibit enriched olefin content in the liquid products.

Another explanation for the higher olefin selectivity in SC-FTOC could involve a suppression of oligomerization in the presence of the supercritical medium. However, this is not consistent with the positive effect of pressure on ASA-catalyzed

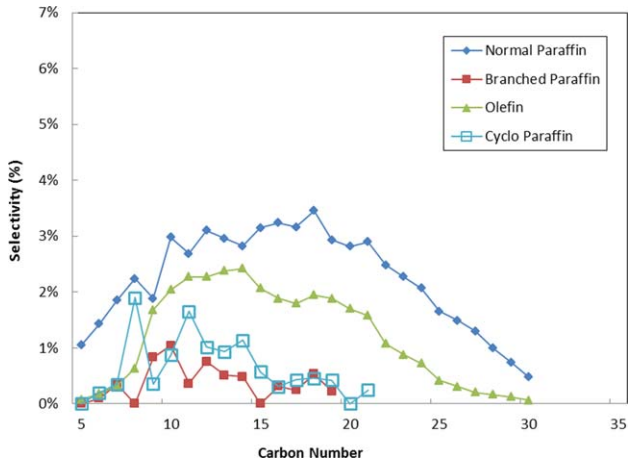

Figure 9. Liquid products selectivities from supercritical phase FTS with subsequent oligomerization and hydrocracking/isomerization stages (SC-FTOC).

[Color figure can be viewed in the online issue, which is available at wileyonlinelibrary.com.]

oligomerization as observed by de Klerk.[40] But, it should be noted that the tests done by de Klerk were performed using a fluidized bed reactor under gas phase feed conditions.

The normal paraffin selectivity was increased from 24.0% in GP-FT to 47.9% in GP-FTOC due to the introduction of the hydrocracking reaction bed (on the 1 wt % Pd/ASA catalyst) which brings about hydrogenation of olefinic products and other unsaturated hydrocarbons. The noble metal, in this case palladium, mainly contributes to hydrogenation as it is active toward electron transfer.[39] The difference in the normal paraffin selectivities between the SC-FT (57.6%) and the GP-FT (24.0%), and between the SC-FTOC (53.8%) and the GP-FTOC (47.9%) indicate that the supercritical phase operations exhibit higher hydrogenation activity. As widely discussed in other supercritical phase FTS literature, contributing factors can include reduced interphase gas–liquid mass transport resistance and enhanced hydrogen diffusivity.[13,63]

Due to the polymerization nature of FT synthesis, it is not particularly selective toward fuel range hydrocarbons. Additionally, the FT fuel that is produced possesses certain quality issues for use as both gasoline and diesel fuel, including poor cold-flow properties (cloud point, pour point, cold filter plugging point, etc.), low lubricity and low density, and so forth.[3,23,63] Increasing the content of branched hydrocarbons in FT fuels can improve these cold-flow properties. Branched hydrocarbons, especially asymmetrical isomers, are more difficult to crystallize than linear paraffins of the same molecular weight, and therefore possess a lower melting point and congealing point than linear paraffins. In addition, asymmetric branched hydrocarbons and most substituted cyclic hydrocarbons contribute to the lubricating capacity of fuels.[84] Yet, the paraffinic hydrocarbons generated from FT synthesis are highly linear. As a result, typically derived FT hydrocarbon fuels that contain low content of branched compounds offer poor cold-flow properties and low lubricity.[21–23] Various fuel additives can be added into the FT fuel blends to improve the cold-flow properties and lubricity, such as methyl ester.[15,85] Aromatics can be used to increase the fuel density and octane number along with the other fuel additives.[86]

In GP-FTOC, a significant amount of branched paraffin was generated. The branched paraffin selectivity in the GP-FTOC experiment increased from 16.3% in GP-FT up to 31.2% by adding the hydrocracking/isomerization stage. The branched paraffin types that were collected in GP-FTOC include 2-methyl-, 3-methyl-, 4-methyl-, 2-dimethyl-, 2,3-dimethyl, 4-ethyl-, and so forth. For the fuel range (C_5—C_{22}), the branched paraffin selectivity was significantly promoted. In SC-FTOC, the presence of the supercritical solvent allows for efficient extraction of reaction intermediates and products (as was also the case in SC-FT),[68] such that cyclo-paraffins (1-R, 2-R, cyclo-propanes) and more olefins were collected as reaction intermediates from the cracking/isomerization reactor bed. This observation is consistent with the mechanisms described by Park and Ihm.[87] It is well recognized that isomerization of *n*-paraffins is the first reaction step in this process while cracking is a subsequent reaction. Monobranched paraffins show a lower tendency toward cracking than multibranched paraffins.[22] The bifunctional catalysts commonly used for hydrocracking/isomerization often contain metallic sites (for hydrogenation/dehydrogenation) and acid sites (for skeletal isomerization via carbenium ions),[22,33,39] in this case, Pd and ASA, respectively. In this study, the SC-FTOC results are consistent with the Park and Ihm mechanism[87] by having exhibited the presence of cyclo-paraffins (1-R, 2-R, cyclo-propanes) and the enhanced olefin selectivity. Note that there were negligible amounts of these cyclo-paraffins observed in GP-FT and GP-FTOC and the amounts were not significant for effective quantification.

Although the isomer selectivity (isomerization activity) was substantial, the cracking of long chain hydrocarbons (C_{22+}) was insignificant when comparing GP-FTOC with GP-FT. Yet, the C_{22+} product selectivity was higher in GP-FTOC than that in GP-FT, which suggests that the oligomerization activity was high for middle range compounds that were converted into C_{22+} products to an extent greater than the cracking of the C_{22+} compounds. However, the GP-FTOC C_{26+} product selectivity (0.1%, not listed in Table 2) was lower than that in GP-FT (0.3%, not listed in Table 2), which means that hydrocracking using this Pd/ASA catalyst under these gas phase conditions favors the cracking of the heavier hydrocarbons (C_{26+}). This result is consistent with the observation that the heavier hydrocarbons are more likely to be involved in cracking.[22] Under supercritical phase conditions, the selectivity of C_{22+} compounds in SC-FTOC was 10.1% compared to 13.6% in SC-FT, thereby illustrating the impact of having introduced the hydrocracking stage. It is important to note that the production of C_{22+} hydrocarbons was greater in SC-FT than in GP-FT, as described above, yet the activity of the hydrocracking stage under supercritical conditions was sufficient to lower the overall C_{22+} hydrocarbon selectivity. The balance between cracking and isomerization can be modified to further affect the product distribution by adjusting the catalyst for hydrogenation/dehydrogenation activity (noble metal) vs. the isomerization activity (acid sites).[39,43]

There were some aromatics produced in the gasoline and jet fuel range in the GP-FTOC experiment, which can enhance the density of the derived FT fuels. Identified aromatics ranged from C_7—C_{12}, including toluene, ethylbenzene, p-xylene, o-xylene, 1-ethyl, 3-methyl-benzene, 1,3,5-trimethyl-benzene, 1,3-diethyl-benzene, 1-methyl,4-propyl-benzene, 1-methyl, 4-(1-methylethyl)-benzene, pentamethyl-benzene, and so forth. Quantitatively, the aromatics concentration (as identified by GC-MS) was approximately 35% of the C_7—C_{12} hydrocarbons (not shown in Table 2). However, the generation of aromatics was only observed in the GP-FTOC operation. Potential contributing factors are that the aromatization process was suppressed thermodynamically or that the concentrations of reactants for aromatization were too low such that there were no distinguishable aromatics generated under supercritical phase conditions.

In examining the liquid products as a function of carbon number, it can be validated that gasoline range (C_5—C_{11}) products was dominate in GP-FT while diesel range (C_{12}—C_{22}) was more prominent in GP-FTOC. In both SC-FT and SC-FTOC, the selectivity toward liquid products was greatly enhanced due to lower production of gas phase products. This is especially true for SC-FTOC where the fuel range products were further intensified through higher selectivity toward gasoline range and diesel range products and less heavy hydrocarbon (C_{22+}) production compared to SC-FT.

Conclusions

This study demonstrates that FTS with subsequent oligomerization and hydrocracking/isomerization stages (FTOC) can be effectively performed using a newly designed three-bed catalytic reactor system. This integrated FTOC process provides opportunities to effectively modify the FTS product. The selectivity toward long chain hydrocarbons (C_{26+}) was diminished due to the introduction of the hydrocracking stage. The liquid product C_{5+} olefin selectivity was observed to be greatly reduced in GP-FTOC compared to GP-FT. The selectivity toward branched paraffins was significantly promoted through the implementation of the hydrocracking and isomerization stages in the GP-FTOC. In addition, appreciable amounts of aromatics were produced in the gasoline and jet fuel range (C_5—C_{15}) in the GP-FTOC. Overall, this work demonstrates that the resulting product distribution can be distinguishably modified toward fuel range products (C_5—C_{22}) in GP-FTOC through the integration of the oligomerization and hydrocracking/isomerization stages immediately subsequent to FTS.

The utilization of SCF media (in this case supercritical hexanes) in FTS was shown to reduce the selectivity toward CH_4 and CO_2 compared to GP-FT. Moreover, SC-FT resulted in a shift in the product distribution toward longer chain hydrocarbons along with an enhanced normal paraffin selectivity compared to GP-FT. Additionally, a significant concentration of aldehyde was detected in the SC-FT liquid products. In the case of SC-FTOC, higher concentrations of cyclo-paraffins (1-R, 2-R, cyclo-propane) and olefins were observed in the liquid effluent. The selectivity toward C_{22+} hydrocarbons was distinguishably less under SC-FTOC conditions compared to SC-FT. Overall, this work illustrates that the selectivity toward transportation fuel range hydrocarbons can be enhanced in SC-FTOC while simultaneously reducing the selectivity toward the undesired products of CH_4 and CO_2.

Acknowledgments

The authors gratefully acknowledge the financial support from the U.S. Department of Energy (grant No. EE0003115), the U.S. Department of Energy (grant No. D-

FC26-05NT42456 through the Consortium for Fossil Fuel Science) and the U.S. Department of Agriculture (grant No. 2011-67009-20077). The authors would like to thank Brian Schwieker and Kenneth Hornsby for their assistance in the development and maintenance of the reactor and analytical system. This contribution was identified by Paul Witt (US Department of Energy.) as the Best Presentation in the session "Syngas Production and Gas-To-Liquid Technology" of the 2012 AIChE Annual Meeting in Pittsburgh, PA.

Literature Cited

1. Lynd LR, Larson E, Greene N, Laser M, Sheehan J, Dale BE, McLaughlin S, Wang M. The role of biomass in America's energy future: framing the analysis. *Biofuels, Bioproducts & Biorefining*. 2009;3(2)113–123.
2. Elbashir NO, Bukur DB, Durham E, Roberts CB. Advancement of Fischer-Tropsch synthesis via utilization of supercritical fluid reaction media. *AIChE J*. 2010;56(4):997–1015.
3. Van der Laan GP, Beenackers AACM. Kinetics and selectivity of the fischer–tropsch synthesis: a literature review. *Catal Rev*. 1999; 41(3&4):255–318.
4. U.S. Dept. of Energy, Gasification-based fuels and electricity production from biomass, without and with carbon capture and storage. Project Report, Project ID 226, http://www.hydrogen.energy.gov/analysis_repository/project.cfm/PID=226, DOE, Hydrogen and Fuel Cells Program, Oct. 2005.
5. Dry ME. Commercial conversion of carbon monoxide to fuels and chemicals. *J Organometal Chem*. 1989;372:117–127.
6. Dry ME. Fischer–Tropsch reactions and the environment. *Appl Catal A: General*. 1999;189(2):185–190.
7. Dry ME. The Fischer – Tropsch process:1950–2000. *Catal Today*. 2002;71:227–241.
8. Davis BH. Fischer-Tropsch synthesis: relationship between iron catalyst composition and process variables. *Catal Today*. 2003;84(1–2): 83–98.
9. Iglesia E. Design, synthesis, and use of cobalt-based Fischer-Tropsch synthesis catalysts. *Appl Catal A: General*. 1997;161(1–2):59–78.
10. Bukur DB, Sivaraj C. Supported iron catalysts for slurry phase Fischer – Tropsch synthesis. *Appl Catal A: General*. 2002;231:201–214.
11. Steynberg AP, Espinoza RL, Jager B, Vosloo AC. High temperature Fischer – Tropsch synthesis in commercial practice. *Appl Catal A: General*. 1999;186:41–54.
12. Schulz H, Riedel T, Schaub G. Fischer–Tropsch principles of cohydrogenation on iron catalysts. *Top Catal*. 2005;32(3–4):117–124.
13. Subramaniam B. Enhancing the stability of porous catalysts with supercritical reaction media. *Appl Catal A: General*. 2001;212(1–2): 199–213.
14. Durham E, Zhang S, Roberts C. Diesel-length aldehydes and ketones via supercritical Fischer Tropsch synthesis on an iron catalyst. *Appl Catal A: General*. 2010;386(1–2):65–73.
15. Huang X, Roberts CB. Selective Fischer–Tropsch synthesis over an Al2O3 supported cobalt catalyst in supercritical hexane. *Fuel Processing Technol*. 2003;83(1-3):81–99.
16. Guo X, Liu G, Larson ED. High-octane gasoline production by upgrading low-temperature Fischer–Tropsch Syncrude. *Ind Eng Chem Res*. 2011;50(16):9743–9747.
17. De Klerk A. Thermal upgrading of Fischer−Tropsch olefins. *Energy Fuels*. 2005;19(4):1462–1467.
18. Eilers J, Posthuma SA, Sie ST. The shell middle distillate synthesis process (SMDS). *Catal Lett*. 1990;7:253–270.
19. Hamelinck CN, Faaij APC, Den Uil H, Boerrigter H. Production of FT transportation fuels from biomass; technical options, process analysis and optimisation, and development potential. *Energy*. 2004; 29(11):1743–1771.
20. Liu G, Larson ED, Williams RH, Kreutz TG, Guo X. Making Fischer−Tropsch fuels and electricity from coal and biomass: performance and cost analysis. *Energy Fuels*. 2011;25(1):415–437.
21. Leckel D. Low-pressure hydrocracking of coal-derived Fischer−-Tropsch waxes to diesel. *Energy Fuels*. 2007;21(3):1425–1431.
22. Calemma V, Gambaro C, Parker WO, Carbone R, Giardino R, Scorletti P. Middle distillates from hydrocracking of FT waxes: Composition, characteristics and emission properties. *Catal Today*. 2010;149(1–2):40–46.
23. Steynberg A, Dry ME, editors. *Fischer-Tropsch Technology*. Studies in Surface Science and Catalysis 152, New York, NY: Elsevier Science Pub. Co., 2004.
24. Morales F, Weckhuysen BM. Promotion effects in co-based Fischer – Tropsch catalysis. *Catalysis*. 2006;19:1–40.
25. Li X, Liu X, Liu Z-W, Asami K, Fujimoto K. Supercritical phase process for direct synthesis of middle iso-paraffins from modified Fischer–Tropsch reaction. *Catal Today*. 2005;106(1–4):154–160.
26. Li X, Asami K, Luo M, Michiki K, Tsubaki N, Fujimoto K. Direct synthesis of middle iso-paraffins from synthesis gas. *Catal Today*. 2003;84(1–2):59–65.
27. Zhang Q, Kang J, Wang Y. Development of novel catalysts for Fischer-Tropsch synthesis: tuning the product selectivity. *ChemCatChem*. 2010;2(9):1030–1058.
28. He J, Yoneyama Y, Xu B, Nishiyama N, Tsubaki N. Designing a capsule catalyst and its application for direct synthesis of middle isoparaffins. *Langmuir*. 2005;21(5):1699–1702.
29. Cho KM, Park S, Seo JG, Youn MH, Baeck SH, Jun KW, Chung JS, Song IK. Production of middle distillate in a dual-bed reactor from synthesis gas through wax cracking: Effect of acid property of Pd-loaded solid acid catalysts on the wax conversion and middle distillate selectivity. *Appl Catal B: Environ*. 2008;83(3–4):195–201.
30. Liu Z-W, Li X, Asami K, Fujimoto K. Iso-paraffins synthesis from modified Fischer–Tropsch reaction—Insights into Pd/beta and Pt/beta catalysts. *Catal Today*. 2005;104(1):41–47.
31. Liu Z-W, Li X, Asami K, Fujimoto K. High performance Pd/beta catalyst for the production of gasoline-range iso-paraffins via a modified Fischer–Tropsch reaction. *Appl Catal A: General*. 2006; 300(2):162–169.
32. Ngamcharussrivichai C, Liu X, Li X, Vitidsant T, Fujimoto K. An active and selective production of gasoline-range hydrocarbons over bifunctional Co-based catalysts. *Fuel*. 2007;86(1–2):50–59.
33. Liu Z-W, Li X, Asami K, Fujimoto K. Selective production of isoparaffins from syngas over Co/SiO2 and Pd/beta hybrid catalysts. *Catal Commun*. 2005;6(8):503–506.
34. Ge Q, Li X, Kaneko H, Fujimoto K. Direct synthesis of LPG from synthesis gas over Pd–Zn–Cr/Pd-β hybrid catalysts. *J Mol Catal A: Chem*. 2007;278(1–2):215–219.
35. Martinez A, Rollan J, Arribas MA, Cerqueira HS, Costa AF, S.-aguiar EF. A detailed study of the activity and deactivation of zeolites in hybrid Co/SiO2-zeolite Fischer–Tropsch catalysts. *J Catal*. 2007;249(2):162–173.
36. Li X, Feng X, Ge Q, Fujimoto K. Direct synthesis of iso-paraffins from syngas with slurry phase reaction. *Fuel*. 2008;87(4-5):534–538.
37. Tsubaki N, Yoneyama Y, Michiki K, Fujimoto K. Three-component hybrid catalyst for direct synthesis of isoparaffin via modified Fischer–Tropsch synthesis. *Catal Commun*. 2003;4(3):108–111.
38. Bessel S. Investigation of bifunctional zeolite supported cobalt Fischer-Tropsch catalysts. *Appl Catal A: General*. 1995;126(95): 235–244.
39. Deldari H. Suitable catalysts for hydroisomerization of long-chain normal paraffins. *Appl Catal A: General*. 2005;293:1–10.
40. De Klerk A. Oligomerization of Fischer−Tropsch olefins to distillates over amorphous silica−alumina. *Energy Fuels*. 2006;20(5): 1799–1805.
41. De Klerk A. Effect of oxygenates on the oligomerization of Fischer−Tropsch olefins over amorphous silica−alumina. *Energy Fuels*. 2007;21(2):625–632.
42. Ancheyta J, Sánchez S, Rodríguez M a. Kinetic modeling of hydrocracking of heavy oil fractions: A review. *Catal Today*. 2005; 109(1–4):76–92.
43. Calemma V, Peratello S, Perego C. Hydroisomerization and hydrocracking of long chain n-alkanes on Pt/amorphous SiO2–Al2O3 catalyst. *Appl Catal A: General*. 2000;190:207–218.
44. Archibald RC, Greensfelder BS, Holzman G, Rowe DH. Catalytic hydrocracking of aliphatic hydrocarbons. *Ind Eng Chem*. 1960;52(9): 745–750.
45. Carter J, Cusumano JA, Sinfelt JH. Hydrogenolysis of n-heptane over unsupported metals. *J Catal*. 1971;20(2):223–229.
46. De Klerk A. Properties of synthetic fuels from H-ZSM-5 oligomerization of Fischer–Tropsch type feed materials. *Energy Fuels*. 2007; 21(6):3084–3089.
47. Subramaniam B, McHugh MA. Reactions in supercritical fluids - a review. *Ind Eng Chem Process Des Develop*. 1986;25(1):1–12.
48. Xu R, Zhang S, Roberts CB. Mixed alcohol synthesis over a K promoted $Cu/ZnO/Al_2O_3$ catalyst in supercritical hexanes. *Ind Eng Chem Res*. 2013;52(41):14514–14524.

49. Xu R, Zhang S, Stewart C, Durham E, Eden MR, Roberts CB. Effect of reaction conditions on supercritical hexanes mediated higher alcohol synthesis over a Cu/Co/Zn catalyst. *AIChE J*. In press.
50. Chester TL, Pinkston JD, Raynie DE. Supercritical fluid chromatography and extraction. *Anal Chem*. 1998;70(12):301–320.
51. Mc Clain J. Processing with supercritical solvents. *Chem Eng*. 107(2):72–79.
52. Linghu W, Li X, Asami K, Fujimoto K. Supercritical phase Fischer?Tropsch synthesis over cobalt catalyst. *Fuel Process Technol*. 2004;85(8–10):1121–1138.
53. Linghu W, Li X, Fujimoto K. Supercritical and near-critical Fischer-Tropsch synthesis: Effects of solvents. *J Fuel Chem Technol*. 2007; 35(1):51–56.
54. Elmalik EE, Tora E, El-Halwagi M, Elbashir NO. Solvent selection for commercial supercritical Fischer–Tropsch synthesis process. *Fuel Process Technol*. 2011;92(8):1525–1530.
55. Jacobs G, Chaudhari K, Sparks D, et al. Fischer–Tropsch synthesis: supercritical conversion using a Co/Al2O3 catalyst in a fixed bed reactor. *Fuel*. 2003;82(10):1251–1260.
56. Abbaslou RMM, Mohammadzadeh JSS, Dalai AK. Review on Fischer–Tropsch synthesis in supercritical media. *Fuel Process Technol*. 2009;90(7–8):849–856.
57. Biquiza LD, Claeys M, Van Steen E. Thermodynamic and experimental aspects of "supercritical" Fischer–Tropsch synthesis. *Fuel Process Technol*. 2010;91(10):1250–1255.
58. Fujimoto K, Yokota K. Supercritical-phase Fischer-Tropsch synthesis reaction. 2. The effective diffusion of reactant and products in the supercritical-phase reaction. *Ind Eng Chem Res*. 1991;(30):95–100.
59. Elbashir NO, Roberts CB. Selective control of hydrocarbon product distribution in supercritical phase Fischer-Tropsch synthesis, *Preprint Paper: ACS*, *Div Pet Chem*. 2004;49(4):422–425.
60. Bukur DB, Lang X, Akgerman A, Feng Z. Effect of process conditions on olefin selectivity during conventional and supercritical Fischer−Tropsch synthesis. *Ind Eng Chem Res*. 1997;36(7):2580–2587.
61. Liu X, Linghu W, Li X, Asami K, Fujimoto K. Effects of solvent on Fischer–Tropsch synthesis. *Appl Catal A: General*. 2006;303(2):251–257.
62. Joyce PC, Leggett BE, Thies MC. Vapor–Liquid equilibrium for model Fischer–Tropsch waxes (hexadecane, 1-hexadecene, and 1-hexadecanol) in supercritical hexane. *Fluid Phase Equilibria*. 1999; 158–160:723–732.
63. Bochniak DJ, Subramaniam B. Fischer-Tropsch synthesis in near-critical n-hexane: Pressure-tuning effects. *AIChE J*. 1998;44(8): 1889–1896.
64. Yokota K, Hnakata Y, Fujimoto K. Supercritical phase Fischer-Tropsch synthesis. *Chem Eng Sci*. 1990;45(8):2743–2749.
65. Yokota K, Fujimoto K. Supercritical phase Fischer-Tropsch synthesis reaction. *Fuel*. 1989;68(2):255–256.
66. Elbashir NO, Roberts CB. Enhanced incorporation of α-olefins in the Fischer−Tropsch synthesis chain-growth process over an alumina-supported cobalt catalyst in near-critical and supercritical hexane medium. *Ind Eng Chem Res*. 2005;44:505–521.
67. Yan S, Fan L, Zhang Z, Zhou J, Fujimoto K. Supercritical-phase process for selective synthesis of heavy hydrocarbons from syngas on cobalt catalysts. *Appl Catal A: General*. 1998;171(2):247–254.
68. Fan L, Fujimoto K. Fischer–Tropsch synthesis in supercritical fluid: characteristics and application. *Appl Catal A: General*. 1999; 186(1–2):343–354.
69. Lang X, Akgerman A, Bukur DB. Steady State fischer-tropsch synthesis in supercritical propane. *Ind Eng Chem Res*. 1995;34(1):72–77.
70. Yokota K, Hanakata Y, Fujimoto K. Supercritical phase Fischer-Tropsch synthesis reaction: 3. Extraction capability of supercritical-fluids. *Fuel*. 1991;70(8):989–994.
71. Soled SL, Iglesia E, Fiato RA, Baumgartner JE, Vroman H, Miseo S. Control of metal dispersion and structure by changes in the solid-state chemistry of supported cobalt Fischer–Tropsch catalysts. *Top Catal*. 2003;26(1–4):101–109.
72. Iglesia E, Reyes SC, Madon RJ, Soled SL. Selectivity control and catalyst design in the Fischer-Tropsch synthesis: sites, pellets, and reactors. *Adv Catal*. 1993;39:221–302.
73. Dry ME. Fischer-Tropsch synthesis over iron catalysts. *Catal Lett*. 1990;7(1–4):241–251.
74. Duvenhage DJ, Espinoza RL, Coville NJ. Fischer-Tropsch precipitated iron catalysts: Deactivation studies. In: Delmon B, Froment GF, edirors. Catalyst Deactivation. 1994:351–358.
75. Duvenhage D, Coville N. Deactivation of a precipitated iron Fischer–Tropsch catalyst—A pilot plant study. *Appl Catal A: General*. 2006;298:211–216.
76. Saib AM, Moodley DJ, Ciobîcăb IM, Haumana MM, Sigwebelaa BH, Weststratec CJ, Niemantsverdrietc JW, van de Loosdrecht J. Fundamental understanding of deactivation and regeneration of cobalt Fischer–Tropsch synthesis catalysts. *Catal Today*. 2010; 154(3–4):271–282.
77. Nlemantsverdrlet JW, Van Der Kraan AM. Behavior of metallic iron catalysts during fischer-tropsch synthesis studied with mbssbauer spectroscopy, X-ray diffraction, carbon content determlnation, and reaction kinetic measurements. *J Phys Chem*. 1980;84:3363–3370.
78. Bukur DB, Koranne M, Lang X, Rao KRPM, Huffman GP. Pretreatment effect studies with a precipitated iron Fischer-Tropsch catalyst. *Appl Catal A: General*. 1995;126(1):85–113.
79. Bukur DB, Lang X. Highly active and stable iron Fischer−Tropsch catalyst for synthesis gas conversion to liquid fuels. *Ind Eng Chem Res*. 1999;38(9):3270–3275.
80. Bukur DB, Okabe K, Rosynek MP, Li CP, Wang DJ, Rao KRPM, Huffman GP. Activation studies with a precipitated iron catalyst for Fischer-Tropsch synthesis I. Characterization studies. *J Catal*. 1995; 155:353–365.
81. De Smit E, Weckhuysen BM. The renaissance of iron-based Fischer-Tropsch synthesis: on the multifaceted catalyst deactivation behaviour. *Chem Soc Rev*. 2008;37(12):2758–2781.
82. DieselNet, Fuel Regulations. Available at: http://www.dieselnet.com/standards/fuels.php. ECOpoint INC. 2012. Accessed on September 2, 2012.
83. U.S. Environmental Protection Agency, Renewable Fuels: Regulations & Standards. Available at: http://www.epa.gov/oms/fuels/renewablefuels/regulations.htm. EPA, Office of Transportation and Air Quality. Accessed on September 2, 2012.
84. Trimm DL, Akashah S, Absi-Halabi M, Bishara A. editors. *Catalysts in Petroleum Refining 1989*. New York, NY; Elsevier Science Pub. Co., 1990.
85. Duvenhage DJ, Shingles T. Synthol reactor technology development. *Catal Today*. 2002;71(2):301–305.
86. De Klerk A. Environmentally friendly refining: Fischer-Tropsch versus crude oil. *Green Chem*. 2007;9(6):560–565.
87. Park KC, Ihm SK. Comparison of Pt/zeolite catalysts for n-hexadecane hydroisomerization. *Appl Catal A: General*. 2000; 203(2):201–209.

Manuscript received Jan. 22, 2014, and revision received Apr. 5, 2014.